Neuron, Vol. 25, 587–597, March, 2000, Copyright ©2000 by Cell Press

The LIM Homeobox Gene *ceh-14* Confers Thermosensory Function to the AFD Neurons in *Caenorhabditis elegans*

Giuseppe Cassata,*# Hiroshi Kagoshima,*# Yoshiki Andachi,‡ Yuji Kohara,‡ Markus B. Dürrenberger,† David H. Hall,§ and Thomas R. Bürglin*‖
*Division of Cell Biology
†Interdepartmental Electron Microscopy
Biozentrum, University of Basel
Klingelbergstrasse 70
CH-4056 BASEL
Switzerland
‡Gene Library Lab
National Institute of Genetics
Mishima 411
Japan
§Center for *C. elegans* Anatomy
Department of Neuroscience
Albert Einstein College of Medicine
Bronx, New York 10461

Summary

In *Caenorhabditis elegans* three pairs of neurons, AFD, AIY, and AIZ, play a key role in thermosensation. The LIM homeobox gene *ceh-14* is expressed in the AFD thermosensory neurons. *ceh-14* mutant animals display athermotactic behaviors, although the neurons are still present and differentiated. Two other LIM homeobox genes, *ttx-3* and *lin-11*, function in the two interneurons AIY and AIZ, respectively. Thus, the three key thermosensory neurons are specified by three different LIM homeobox genes. *ceh-14 ttx-3 lin-11* triple mutant animals have a basic cryophilic thermotaxis behavior indicative of a second thermotaxis pathway. Misexpression of *ceh-14* in chemosensory neurons can restore thermotactic behavior without impairing the chemosensory function. Thus, *ceh-14* confers thermosensory function to neurons.

Introduction

Temperature is a major determinant of an animal's metabolism. As a cold-blooded organism, *Caenorhabditis elegans* has a limited physiological temperature range (~12°C–26°C) at which it is viable and fertile. Thermotaxis behaviors allow animals to track to a preferred temperature. This is due to a basic memory that can last several hours and allows the animal to return to the optimal temperature or to avoid it if starved (Hedgecock and Russell, 1975). The worm is therefore able to sense temperature, to remember it, and to modify its behavior based on previous experience.

The function of both sensory neurons and interneurons in thermotaxis has been analyzed in cell ablation experiments (Mori and Ohshima, 1995). Killing the AFD sensory neurons by laser beam microsurgery leads to a severe athermotactic (nontemperature-responsive) phenotype in some animals and to a cryophilic (cold-seeking) phenotype in others. The AFD cells have finger-like dendritic endings that are completely embedded in sheath cells at the tip of the nose. This great increase of area has been proposed to be important for correct thermosensation (Perkins et al., 1986).

Laser ablation of either the AIY (the only target cells of AFD; White et al., 1986) or the AIZ interneurons leads to less severe, mistactic phenotypes that are interesting because they are opposite to each other: killing AIY causes a cryophilic phenotype, whereas killing AIZ causes a thermophilic (heat-seeking) phenotype (Mori and Ohshima, 1995). Taken together, the laser ablation experiments and the morphological studies (Perkins et al., 1986; White et al., 1986) dissected a thermosensory neuronal network containing one pair of sensory neurons (AFD) and two pairs of interneurons (AIY and AIZ) that is sufficient to sense and integrate thermosensation with other sensory inputs to produce an appropriate motor output.

Although the neuronal connections and the characteristics of the thermosensory neurons and their interneurons are well determined, little is known about molecular factors involved in thermosensation. Two cyclic nucleotide-gated channels (*tax-2* and *tax-4*) were shown to play a role in different types of sensory transduction. They direct chemosensory signals as well as thermosensory cues (Coburn and Bargmann, 1996; Komatsu et al., 1996). Another protein, the guanylyl cyclase GCY-8, is exclusively expressed in AFD thermosensors (Yu et al., 1997), though its function is unknown.

In vertebrates other proteins have been shown to be able to react to temperature at a nociceptive level in cell culture experiments. These are two members of a family of heat-gated ion channels (Caterina et al., 1997, 1999). Whereas the first, the capsaicin receptor VR-1, seems to be heat activated in pain sensation (Caterina et al., 1997), the second, VRL-1, seems to be involved in sensation of noxious heat only and not in chemosensation. However, VRL-1 transcripts are not restricted to sensory neurons, which indicates that the channel might be activated by stimuli other than heat (Caterina et al., 1999). Although a genuine homolog of these two proteins has been found in the worm, OSM-9, it has only been shown to be required for olfaction, mechanosensation, and olfactory adaptation, not for thermosensation at the physiological level (Colbert et al., 1997).

A family of conserved genes playing a crucial role in neuronal survival, axon guidance, neurotransmitter expression, and neuronal function are the LIM homeodomain transcription factors (Way and Chalfie, 1988; Lundgren et al., 1995; Pfaff et al., 1996; Hobert et al., 1997, 1998; Thor and Thomas, 1997). *mec-3* was the first member of this family that was discovered and shown to specify mechanosensory neurons in *C. elegans* (Way and Chalfie, 1988). LIM homeodomain proteins contain several domains, the homeodomain, and two LIM domains. Whereas the homeodomains are DNA

‖To whom correspondence should be addressed (e-mail: thomas.buerglin@unibas.ch).
#These authors contributed equally to this work.

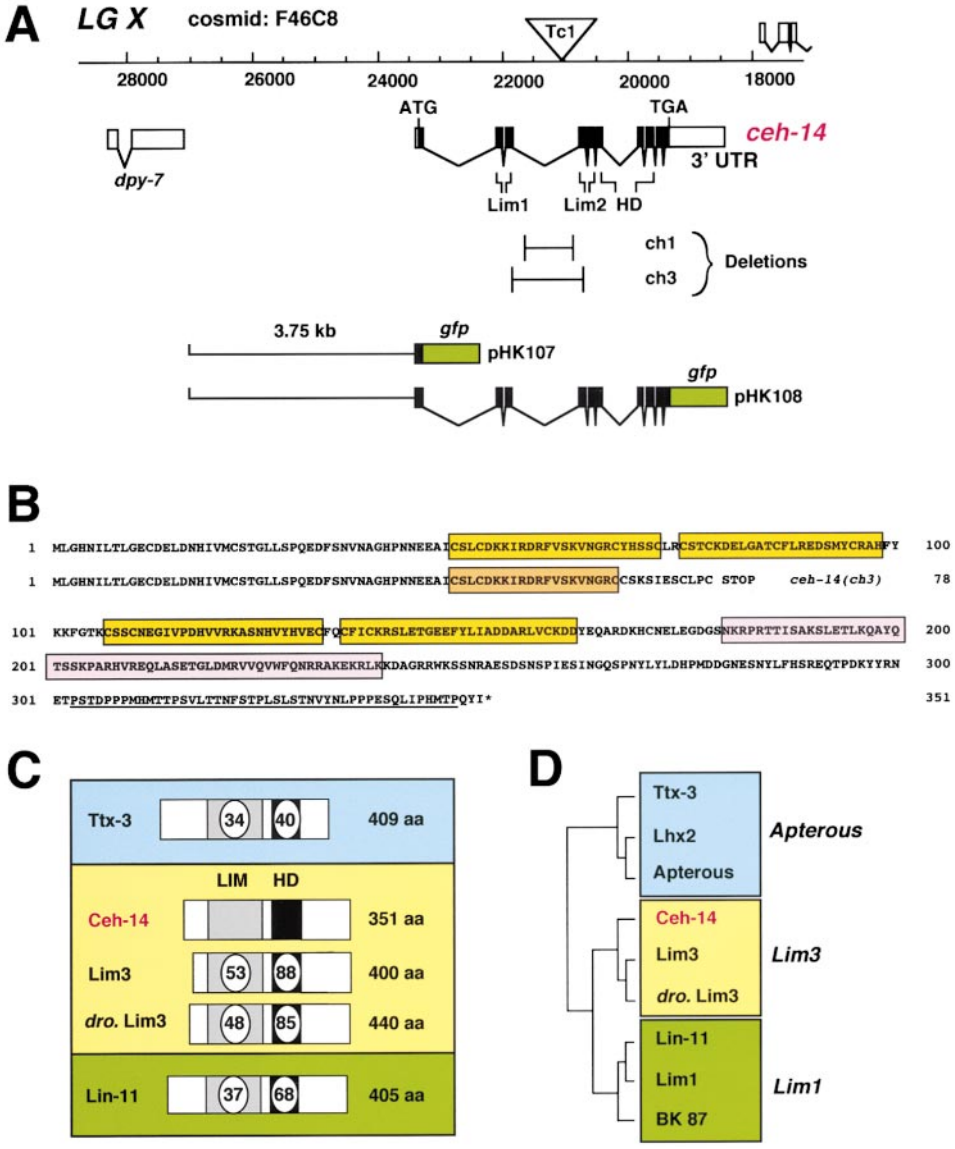

Figure 1. *ceh-14* Gene Structure, Gene Deletions, GFP Reporter Constructs, and Sequence Analysis

(A) *ceh-14* gene structure: the intron/exon structure of *ceh-14* is shown underneath cosmid F46C8 on linkage group X. The insertion point of the Tc1 transposable element is marked with an arrow at position 20945. The two deletions *ch1* and *ch3* are indicated. The structure of the GFP reporter constructs pHK-107 and pHK-108 is shown underneath.

(B) Amino acid sequence of *ceh-14*. The two bipartite LIM domains are boxed in yellow, the homeodomain in purple. The resulting protein of *ceh-14(ch3)* is shown with its incomplete first LIM domain (orange), frameshift, and premature stop. The proline-rich putative transactivation domain is underlined.

(C) Schematic structure of worm, fly, and vertebrate LIM homeobox genes showing amino acid identities within the LIM domains and homeodomains.

(D) Dendrogram of selected LIM homeodomain sequences showing the relationship of the three gene families involved in thermosensation in the worm. TTX-3, CEH-14, and LIN-11 are *C. elegans* proteins. Apterous, *dro*. Lim3, and BK87 are *Drosophila* proteins. BK87 is a partially characterized LIM homeobox gene obtained from DNA-binding studies (Kalionis and O'Farrell, 1993). Lhx2, Lim3, and Lim1 are from vertebrates. These LIM homeobox genes are subdivided in the three subclasses Apterous, Lim3 (LHX3/4), and Lim1 (LHX1/5) according to Dawid et al. (1995) and Hobert et al. (1997).

binding, the LIM domains are zinc-binding motifs interfacing with other proteins (Agulnick et al., 1996; Jurata et al., 1996; Bach et al., 1997; Dawid et al., 1998). In the chick and zebrafish nervous system, combinatorial expression of the four LIM homeodomain proteins Isl1, Isl2, Lim1, and Lim3 mark differentiated subsets of motor neurons (Tsuchida et al., 1994; Appel et al., 1995; Varela-Echavarria et al., 1996). Recently, it was found in *Drosophila melanogaster* that a combinatorial code composed of the two LIM homeodomain proteins Lim3 and Islet determines the motor neuron pathway selection (Thor et al., 1999). Similarly, the specification of ventral motor neuron pathway selection versus dorsal pathway selection in mouse is determined by the mouse homologs of *lim3*, *Lhx3* and *Lhx4* (Sharma et al., 1998). In *Drosophila* as well as in mouse, misexpression of

lim3 or *Lhx3*, respectively, is sufficient to redirect the motoneural axonal projection.

Here we present the expression and mutational analysis of the *C. elegans* ortholog of *Lhx3* and *Lhx4*, *ceh-14*.

Results

ceh-14 Encodes a LIM Homeodomain Protein

The homeodomain of *ceh-14* was previously cloned using degenerate oligonucleotides (Bürglin et al., 1989). For further study, the genomic locus of cosmid XXF4 was sequenced. This contained the complete predicted open reading frame (ORF). The overlapping cosmid F46C8 has now been completely sequenced by the *C. elegans* genome project (*C. elegans* Sequencing Consortium, 1998; Figure 1A). Using primers for the 5′ and 3′ ends of the ORF, a *ceh-14* cDNA was isolated and used to screen and isolate full-length *ceh-14* cDNA clones. These cDNAs confirmed that the gene is composed of 10 exons distributed over 5 kb (Figure 1A).

The putative protein product of 351 amino acids contains two LIM domains and a homeodomain typical for LIM homeodomain transcription factors (Figure 1B; reviewed by Dawid et al., 1995). Furthermore, a proline-rich putative transactivation domain is present at the carboxyl terminus (Figure 1B). Sequence alignments show that CEH-14 has 85%–88% identity within the homeodomain and 48%–53% identity within the LIM domains to the mouse Lhx3 and Lhx4 proteins and to Lim3 of *Drosophila* (Figure 1C). Phylogenetic analysis of the CEH-14 homeodomain (Bürglin, 1995) shows that *ceh-14* belongs to the LHX3/4 family of LIM homeobox genes (Figure 1D). Furthermore, *ceh-14* is the only LHX3/4-type gene in *C. elegans*, which confirms that *ceh-14* is the ortholog of the vertebrate LHX3/4 and *Drosophila lim3* genes.

ceh-14 Is Expressed in the AFD Thermosensory Neurons

The *ceh-14* expression pattern was analyzed using transgenic animals bearing *ceh-14::gfp* reporter constructs (Figure 1A). Two *ceh-14::gfp* reporter constructs were used that differ in respect to the portion of coding sequence they contain. Whereas pHK-107 contains only the first 16 amino acids, pHK-108 contains the full-length ORF (Figure 1A). In addition, a specific rabbit antiserum was raised against a CEH-14 fusion protein to independently confirm the expression (see Experimental Procedures).

GFP expression in the anterior was observed in the sensory neurons AFDL/R, in the interneurons BDUL/R, and in the asymmetrical interneuron ALA (Figures 2A and 2B). The expression pattern of the GFP constructs was continuous from the late embryonic through all larval stages and maintained in adults. Both constructs show the same expression pattern. Larval and adult expression of CEH-14 protein in AFDL/R and BDUL/R was confirmed by immunolocalization (Figures 2C and 2D, and data not shown) using the CEH-14-specific antiserum. One additional cell expressing CEH-14 was observed in the head, at a location consistent with that for ALA (data not shown). The staining was always nuclear, as expected of a DNA-binding transcription factor. We conclude that the GFP reporter constructs and the immunolocalization reflect the bona fide expression pattern of *ceh-14* through larval and adult stages.

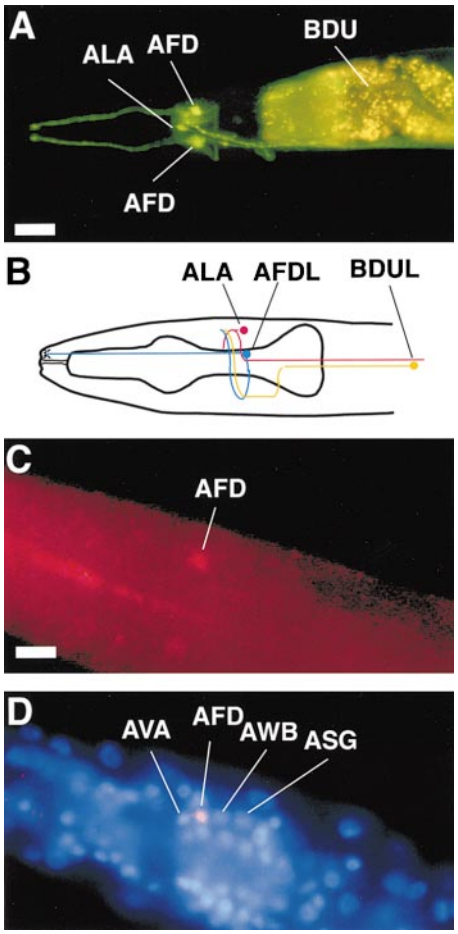

Figure 2. Expression Analysis of *ceh-14*

(A) Fluorescent photomicrographs of a transgenic adult hermaphrodite carrying pHK-108 and the *rol-6* marker, which causes a twisted body: the anterior to the left shows a dorsal-ventral view, the central region a more lateral view. The cells expressing CEH-14::GFP are the thermosensory neurons AFDL/R, the interneurons BDUL/R, and the asymmetric interneuron ALA. These cells were identified on their characteristic morphology and the position of their nuclei viewed by simultaneous fluorescence and Nomarski differential interference microscopy. Scale bar, 40 μm.

(B) Schematic drawing of the cells expressing *ceh-14* in the head, lateral view.

(C) Immunolocalization using anti-CEH-14 serum: the antibody detects AFD as well as the other neurons expressing CEH-14 (data not shown). Scale bar for (C) and (D), 12 μm.

(D) Superposition of antibody immunolocalization and DAPI nuclear staining of the same animal. The antibody staining is nuclear, confirming that *ceh-14* is a transcription factor and localized as expected.

In the tail region, *ceh-14* is expressed in PVT, PVQL/R, DVC, PVNL/R, PVWL/R, PVR, PHCL/R, PHAL/R, and PHBL/R.

ceh-14 Loss-of-Function Mutants are Athermotactic

To investigate the function of *ceh-14*, a Tc1 transposon insertion in intron 3 of the *ceh-14* locus was isolated (Figure 1A). Two deletions were derived from this insertion, called *ceh-14(ch1)* and *ceh-14(ch3)*. *ceh-14(ch1)*

Table 1. Isothermal Tracking Assays of *ceh-14* Mutants, Rescue, and Multiple Mutants

	wt	intermediate	athermotactic	cryophylic	thermophylic	n
N2	94	0	2	3	1	129
ceh-14 (*ch1*)	71	20	2	3	4	93
ceh-14 (*ch3*)	33	22	40	2	3	108
ceh-14(ch3) pHK108[a]	63	18	10	6	3	114
ch3 / N2	76	12	11	0	1	66
ch3 / uDf1	29	25	30	2	14	116
ttx-3 (*ks5*)	3	29	4	64	0	120
lin-11(*n389*)	50	1	12	2	35	82 (8)[b]
TB530 (*ceh-14/ttx-3*)	0	54	29	15	2	99
TB531 (*ttx-3/lin-11*)	0	19	16	63	2	68 (82)[b]
TB532 (*lin-11/ceh-14*)	23	14	26	1	36	90 (10)[b]
TB533 (*triple*)	3	20	26	51	0	72 (28)[b]

[a] The average of four out of six pHK-108 rescuing transgenic lines is shown. Control construct pHK-107 does not rescue (not shown). *ch3/uDf1* is *ceh-14(ch3)* over the *uDf1* deficency: the data show that *ceh-14(ch3)* is a null mutant. *ch3*/N2 heterozygous wild-type animals show only a mild abnormality, consistent with a loss-of-function phenotype.

[b] Several mutant combinations showed significant numbers of animals (indicated in brackets) that were not scored because of poor movement. While most can be attributed to the Unc phenotype of *lin-11* that is unrelated to thermotaxis, *ttx-3/lin-11* animals are particularly immobile.

The different phenotypes of the mutants are shown in percentage. n indicates the number of animals tested; each was only tested once. The standard deviation (Mori et al., 1995: $\pm 2\sqrt{[p(1-p)/n]}$) ranges from 0 to 12 (not shown). Scores relevant for phenotypic analysis are highlighted. The green color stands for wild type, the yellow color for athermotactic, the blue color for cryophilic, the red color for thermophilic, and the green/yellow boxes for intermediate behavior.

deletes only intronic sequences, while *ceh-14(ch3)* deletes intron 3 and produces a frameshift upstream of the second LIM domain and the homeodomain (see Experimental Procedures). Molecular and genetic data show that *ceh-14(ch3)* is a null mutation (see Experimental Procedures).

ceh-14 mutant animals show no morphological defects as judged by light microscopy. Extensive behavioral analysis of the *ceh-14* mutants, including chemotaxis, osmotic avoidance, pharyngeal pumping, egg laying, coordination, touch response, and thermotaxis, revealed only thermotaxis defects (data not shown; see below). Using standard thermotaxis assays (Hedgecock and Russell, 1975; Mori and Ohshima, 1995), we show that a large fraction of *ceh-14(ch3)* animals fail to perform isothermal tracking; nevertheless, 33% are still wild type (Table 1). We distinguished five categories according to Mori and Ohshima (1995) with modifications. These categories are wild type, intermediate (between wild type and athermotactic), athermotactic, cryophilic, and thermophilic. Although *ceh-14(ch1)* has no lesion of the transcript, a slight thermotaxis defect can be observed (Table 1). No difference of *ceh-14* gene expression between wild-type and *ceh-14(ch1)* animals was detected (data not shown), but we cannot exclude a very mild, direct or indirect, regulatory effect only visible at the phenotypic level.

A large percentage of the *ceh-14(ch3)* animals show athermotactic behavior, but some intermediate and wild-type behavior can still be observed (Table 1). Is *ceh-14(ch3)* a null allele? We examined *ceh-14(ch3)* over the chromosomal deficiency (*uDf1*). The hemizygous animals did not show a more severe phenotype (Table 1). Thus, *ceh-14(ch3)* is a true null mutant, and additional factors or cofactors may play a role in thermotaxis. We also examined the phenotype of *ceh-14(ch3)*/wild-type heterozygous animals and found that they displayed an essentially wild-type behavior (Table 1), suggesting that no dominant phenotype results from the deletion.

To demonstrate that the observed phenotypes are due to the deletion in *ceh-14(ch3)*, we introduced *ceh-14::gfp* constructs containing either the full-length coding region of *ceh-14* (pHK-108) or only the first 16 amino acids of *ceh-14* (pHK-107; Figure 1A). The full-length construct was able to rescue *ceh-14(ch3)* animals, whereas pHK-107 was not (Table 1). We conclude that *ceh-14* expression in AFD is required for correct AFD-mediated thermotaxis.

AFD Morphogenesis Is Almost Normal in *ceh-14* Null Mutants

Analysis of *ceh-14(ch3)* mutants carrying pHK-107 indicated already that the AFD neurons are still present. pHK-107 transgenic animals showed normal expression in a *ceh-14(ch3)* background and displayed no apparent malformations in their neuronal processes by light microscopy or changes in GFP intensity in AFD (data not shown). Thus, the AFD neurons are generated and the maintenance of *ceh-14* expression in adults does not require its own gene product, unlike other *C. elegans* LIM homeobox genes such as *ttx-3* and *mec-3* (Way and Chalfie, 1989; Hobert et al., 1997).

The gene *tax-4* encodes a cyclic nucleotide-gated channel, which was shown to be required for correct chemosensation and thermosensation (Coburn and Bargmann, 1996; Komatsu et al., 1996). We crossed wild-type animals carrying a *tax-4::gfp* construct into *ceh-14(ch3)* to analyze possible expressional regulation in

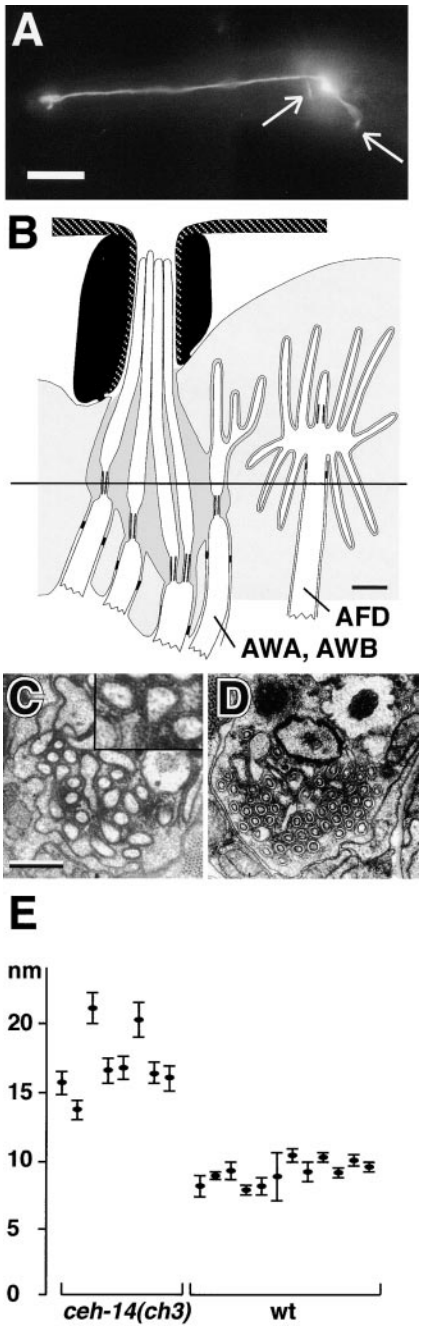

Figure 3. Analysis of AFD Morphology

(A) Fluorescent photomicrograph of an adult *ceh-14(ch3)* hermaphrodite transgenic for the AFD marker *gcy-8::gfp* (Yu et al., 1997). The arrows show the typical axonal "loop" still present in *ceh-14(ch3)*. An enlarged region at the end of the dendrite where the fingers are located can also be seen. Scale bar, 30 μm.

(B) Scheme of an amphid ending showing the different dendritic endings of sensory neurons. A line indicates the level of the electron microscopy section in (C). Modified with permission from Perkins et al. (1986).

(C) Representative electron micrograph section showing the typical AFD dendritic ending of a *ceh-14(ch3)* animal. This horizontal section is about 5 μm from the tip of the nose. The diameters of the *ceh-14(ch3)* mutant AFD fingers have a mean of 17 nm. Scale bar, 1 μm (also for [D]). Also shown is detail enlargement of double membrane of the AFD fingers, demonstrating the presence of the fingers within the indentations in the sheath cell.

AFD. No change in GFP expression level was observed (data not shown).

Next, we generated transgenic lines with a *gcy-8::gfp* reporter construct, which is expressed in the entire AFD cell body and therefore constitutes an ideal marker (Yu et al., 1997). The reporter construct did not reveal any defects in AFD in either wild-type or *ceh-14(ch3)* background. The typical overall morphology was not changed and the axonal loop was always present (White et al., 1986), as judged by light microscopy (Figure 3A). The only postsynaptic partner of AFD is the interneuron AIY (White et al., 1986). Requirement of postsynaptic influence for correct axon formation was tested by analyzing AFD axon morphology in *ttx-3(ks5)* mutants using the *gcy-8::gfp* reporter. *ttx-3* encodes a LIM homeodomain transcription factor that is required for correct neurite morphology in AIY (Hobert et al., 1997). No defects in AFD axon morphology were detected in either *ttx-3(ks5)* or *ceh-14(ch3) ttx-3(ks5)* mutants (data not shown). Thus, *ceh-14* and *ttx-3* are not involved in pre- and/or postsynaptic pathways regulating AFD axonal outgrowth. However, we cannot exclude subtle defects that are difficult to visualize by light microscopy.

The dendritic endings of the AFD neurons constitute a great increase in surface area and might be important for correct thermosensation. In fact, electron microscopy of serial sections of *ttx-1* mutants (which are cryophilic) showed that they lack this typical structure (Perkins et al., 1986). We analyzed whether *ceh-14* is required for correct formation of the AFD dendritic fingers using electron microscopy of serial sections. Eight *ceh-14(ch3)* young adult animals were sectioned at the level of the dendritic endings (around 5 μm from the tip of the nose). The endings were present in 14 out of 16 AFD cells analyzed and showed a generally normal morphology (Figure 3C). However, measurement of the diameter of the dendritic fingers revealed that in *ceh-14(ch3)* mutants the mean diameter is 17 nm, whereas in wild-type animals the finger-like projections measure 10 nm (Figures 3C–3E). In contrast, the number of fingers is reduced by about 25% in *ceh-14(ch3)*. Thus, there is little change in the overall surface area, but fewer fingers are formed, indicating that structural or functional molecules within the fingers are missing or altered. This supports the notion that molecules located in the fingers play an important role in thermosensation, although the presence of fingers per se is not sufficient for proper thermosensation.

Three LIM Homeodomain Proteins Specify the Three Key Neurons for Thermotaxis

The two LIM homeodomain genes *ttx-3* and *lin-11* have been shown to be essential for the function of the interneurons AIY and AIZ, respectively (Hobert et al., 1997, 1998). These data together with ours on *ceh-14* correlate well with the cell ablation experiments performed by

(D) Electron micrograph section of wild-type animals, which show an average diameter of the AFD fingers of 10 nm.

(E) Difference of the mean diameter in AFD fingers between *ceh-14(ch3)* mutants and wild type. Eight *ceh-14(ch3)* mutants and 12 wild-type animals were measured.

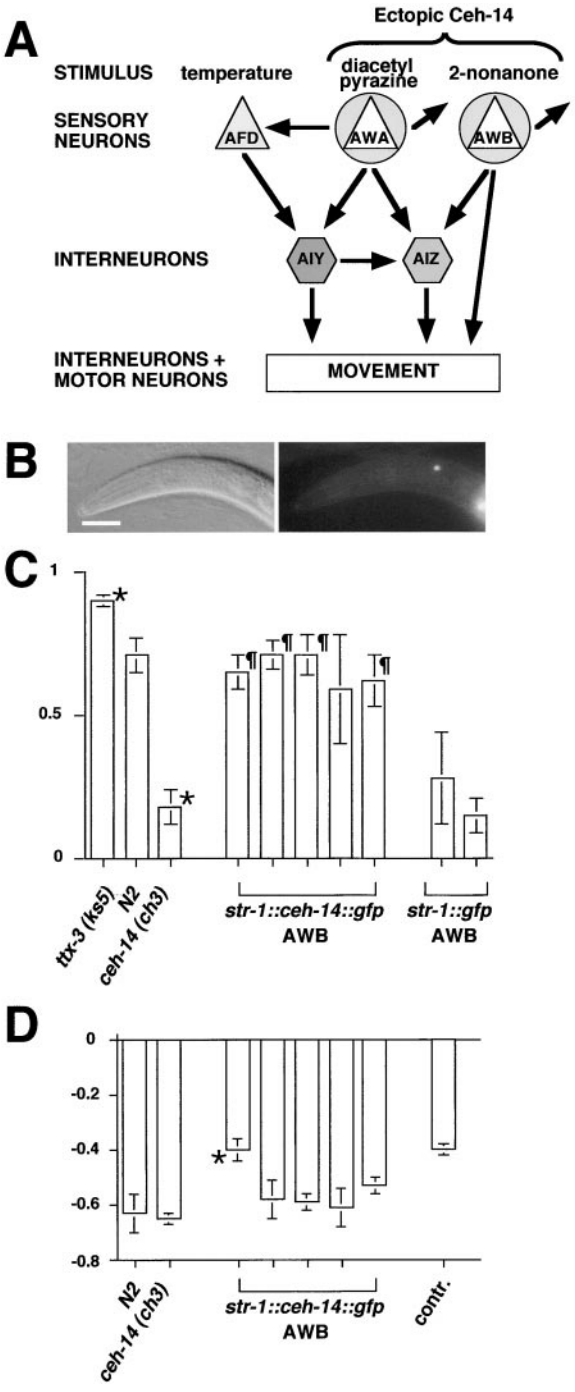

Figure 4. Ectopic Expression of *ceh-14*

(A) Simplified neuronal connectivity scheme showing where *ceh-14* was misexpressed in *ceh-14(ch3)* mutant background animals.

(B) Nomarski and fluorescent photomicrographs of ectopic CEH-14::GFP expression in AWB. The correct expression of *ceh-14* was assayed by the detection of a CEH-14::GFP translational fusion product driven by the AWB cell-specific promotor *str-1* (Troemel et al., 1997). Scale bar, 30 μm.

(C) Bar graph analysis with standard errors of the mean of the thermotaxis indexes obtained from steep thermal gradient assays. The asterisks mark a significant difference of the mutants *ttx-3(ks5)* (cryophilic) and *ceh-14(ch3)* (athermotactic) from wild type (N2). The right part shows thermotaxis indexes of five independent transgenic lines that misexpress *ceh-14* in AWB using the *str-1* promoter. The ¶ sign marks the lines that significantly rescue the athermotactic behavior of the *ceh-14(ch3)* genetic background at $p < 0.01$. The last two transgenic lines are controls carrying *str-1::gfp* only.

(D) The five lines ectopically expressing CEH-14 in AWB were assayed for avoidance to 2-nonanone. "Contr." are wild-type animals adapted for 1 hr to 50% 2-nonanone. Only the line marked with an asterisk (more similar to the control) shows a significant difference from wild type (N2) or *ceh-14(ch3)*, which is also wild type for 2-nonanone avoidance.

Mori and Oshima (1995). Thus, this simple three neuron thermosensory circuit is specified by a distinct three-LIM homeodomain factor system or code. Mori and Oshima also proposed a possible minor role of the AIB interneurons.

We genetically analyzed the thermotaxis behavior of multiple mutants using the three alleles *ceh-14(ch3)*, *ttx-3(ks5)*, and *lin-11(n389)*. In *ceh-14 ttx-3* double mutants a similar amount of animals are athermotactic compared to *ceh-14* (Table 1), but none retain normal behavior. The remainder are either cryophilic or intermediate in these double mutants. In *ceh-14 lin-11* double mutants most animals are thermophilic like in *lin-11*, but the proportion of athermotactic animals has reached almost *ceh-14(ch3)* levels (Table 1). In *ttx-3 lin-11* double mutants the phenotype is rather similar to *ttx-3* alone; thus, *ttx-3* can be considered to be epistatic to *lin-11* (Table 1). Notably, like the laser ablation experiments (Mori and Ohshima, 1995), an unusually large proportion of the animals failed to move, possibly the consequence of conflicting downstream signals, which results in paralysis rather than athermotaxis. Similar to the *ttx-3 lin-11* double mutants, the *ceh-14 ttx-3 lin-11* triple mutants are mainly cryophilic, while the paralysis was partially rescued. This is surprising since one would have expected that impairment of AFD, AIY, and AIZ would result in athermotactic behavior. Our experiments show that even if the key thermosensory circuitry is genetically removed, the animals tend to move to cold, although they do not perform isothermal tracking.

Ectopic Expression of *ceh-14* in Chemosensory Neurons Is Sufficient to Establish Thermosensory Function in *ceh-14(ch3)* Animals

Since *ceh-14* does not play a principal role in the morphogenesis of the AFD neurons, it may regulate expression of genes required for the perception and/or signaling of temperature information. Ectopic expression of CEH-14 in other sensory neurons that are not thermosensory would show whether CEH-14 is sufficient to confer thermosensory function to these cells.

We decided to misexpress *ceh-14* in the chemosensory neuron pairs AWA and AWB for three reasons. First, two cell-specific promoters (for the gene *odr-10* in AWA and *str-1* in AWB) have been described that are suitable for such an experiment (Sengupta et al., 1996; Troemel et al., 1997). Second, AFD, AWA, and AWB share some morphological attributes, such as an enlarged surface at the dendritic endings, and they partially share at least the AIY and AIZ interneurons as postsynaptic partners (White et al., 1986; Figure 4A). Third, AWA and AWB have been shown not to be required for thermotaxis in the presence of AFD (Mori and Ohshima, 1995).

We ectopically expressed the *ceh-14* cDNA fused to *gfp* using either the *odr-10* or the *str-1* promoter in *ceh-14(ch3)* mutant backgrounds. The transgenic lines were examined for correct expression in AWA or AWB using fluorescence microscopy. In both cases, ectopic expression was present and was localized to nuclei as expected (Figure 4B, and data not shown). The animals that ectopically express *ceh-14* were not able to perform isothermal tracking on a radial gradient (data not shown). This is probably due to the different synaptic connectivities of AWA and AWB, which are different from those of the AFD thermosensory system and therefore cannot correctly interpret ectopic thermosensory information.

To overcome this limitation, we developed a modified thermotaxis assay derived from a linear temperature gradient described by Hedgecock and Russell (1975). This assay allows statistical analysis of populations using a thermotaxis index (see Experimental Procedures). With this assay, we obtained significant and reproducible differences of thermotaxis indexes between N2, *ttx-3(ks5)*, and *ceh-14(ch3)* populations (Figure 4C). We then examined five ectopic expression lines for either AWA or AWB. Ectopic expression of CEH-14 in AWA resulted in highly variable thermotaxis indexes, which were mostly not statistically different from the *odr-10::gfp* vector control. This high variability may possibly be due to one of the following: AWA synapses with both AIY and AIZ; transcription factors for the *odr-10* promoter are limiting and are being titrated out by the extrachromosomal arrays; there is a possible difference in neurotransmitters between AFD and AWA; no other LIM-HD is expressed in AWA and therefore required cofactors are missing. Chemosensory assays specific for AWA showed that their chemosensory properties remained wild type (data not shown). We conclude that AWA is not suitable for ectopic expression of CEH-14 and that we see no significant rescue of the athermotactic behavior. In contrast, four out of five lines expressing CEH-14 in AWB have a thermotaxis index similar to wild type and are significantly different ($p < 0.01$) from that of *ceh-14(ch3)* or *ceh-14(ch3)* containing only the *str-1::gfp* reporter (Figure 4B). AWB expresses also *lim-4* (Sagasti et al., 1999) and therefore general cofactors required for LIM-HD proteins are present.

To test whether the AWB underwent transformation, we performed the chemotaxis tests specific for AWB neuronal function (Sengupta et al., 1996; Troemel et al., 1997). We found that the chemotaxis behavior is wild type (Figure 4D), which suggests that the AWB neurons were basically not altered. To examine their morphology, we generated transgenic lines carrying both *str-1::gfp* and *str-1::ceh-14::gfp*. Neuronal processes were examined by confocal microscopy, but no morphological abnormalities were seen. No AFD-specific markers that are regulated by *ceh-14* are known. Nevertheless, we also generated transgenic lines coexpressing the AFD-specific *gcy-8::gfp* marker with the constructs ectopically expressing *ceh-14*. *gcy-8::gfp* expression was only seen in AFD but not in AWB. As expected, ectopic expression of *ceh-14* does not change the identity of these cells, and their morphological features and connectivities important for chemosensory signal transduction are not affected. These experiments show that *ceh-14* is sufficient to confer thermosensory qualities to amphid cells that are not thermosensory.

Discussion

ceh-14 Is Required for Correct AFD-Mediated Thermotaxis

Among several other neurons, the LIM homeobox gene *ceh-14* is expressed in the AFD thermosensory neurons. A large proportion of the *ceh-14* null mutants are athermotactic (Table 1). The incomplete penetrance of the phenotype may be due to additional factors that are necessary for AFD-mediated thermosensation and/or thermotaxis. However, even in the case of laser ablations of AFD, not all animals display athermotactic behavior but rather cryophilic behavior (Mori and Ohshima, 1995; Figure 4A). The athermotactic behavior may not be a consequence of lack of information but may rather be caused by conflicting signaling from AIY, AIZ, and possibly other neurons, when AFD is not functional anymore.

ceh-14 is expressed throughout all larval and adult stages and therefore is probably required for the maintenance of functionality. This has been observed for the other LIM homeobox genes involved in thermosensation, i.e., *ttx-3* and *lin-11* (Hobert et al., 1997, 1998). Positive autoregulatory loops have been shown to be of importance for maintaining the expression of the LIM homeodomain transcription factor MEC-3 (Way and Chalfie, 1989), and TTX-3 (Hobert et al., 1997). However, *ceh-14* is not downregulated in the mutant background.

The overall structure of the AFD thermosensory neurons is only mildly affected in *ceh-14* null mutants (Figure 3), and the markers we examined are still expressed. Thus, *ceh-14* does not play a role in generating AFD but is required for the final differentiation of these neurons. Similarly, it was shown for *mec-3* and other LIM homeodomain proteins that they generally regulate neuronal function and terminal differentiation (Way and Chalfie, 1988; Hobert et al., 1997, 1998). The overall maintenance of wild-type morphology in *ceh-14* mutants suggests that genes regulated by *ceh-14* are only required late in differentiation. The small diameter increase of the AFD fingers in *ceh-14(ch3)* may be an indirect consequence of missing or altered molecules involved in thermosensation, which may change the local regulation of cytoskeletal dynamics. For example, mutations in the cyclic nucleotide-gated channel TAX-2 lead to rather abnormal axon morphology (Coburn et al., 1998).

ceh-14 belongs to the LHX3/4 family of LIM homeodomain proteins (Figure 1B). The fly ortholog *lim3* and the mouse orthologs *Lhx3* and *Lhx4* were shown to be required for axonal pathfinding of motor neurons (Sharma et al., 1998; Thor et al., 1999). Since *ceh-14* is not expressed in motor neurons and since we see no defect in axonal pathfinding in AFD, ALA, or BDU, we conclude that LIM factors do not regulate outgrowth in all neurons expressing them.

We showed that the thermotaxis defects are due to lack of *ceh-14* in AFD. The other neurons are not likely to be responsible for thermosensation as they are not

directly connected with any structure described to be responsible for thermotaxis (Mori and Ohshima, 1995).

Genetic Analysis of the Thermosensory Circuit Uncovers a Second Thermotactic System

In vertebrate and fly motor neurons, combinatorial codes of LIM homeobox genes have been shown to be important for cell identity (Tsuchida et al., 1994; Pfaff et al., 1996; Sharma et al., 1998; Thor et al., 1999). We show that in *C. elegans* the key thermosensory circuit consisting of AFD, AIY, and AIZ is specified by three LIM homeobox genes. We propose that LIM homeobox gene codes are conserved in evolution and that they function in multiple systems, although not always in a combinatorial fashion.

The most striking finding of our genetic analysis of the thermosensory circuit was that none of the double or triple mutants were able to suppress thermotaxis completely. The summary in Figure 5A shows that the triple mutant displays a phenotype similar to that of the laser ablation of AFD. We assume these two phenotypes to be related since both completely uncouple AFD from the motor output and therefore constitute a complete loss of AFD function, even though *ceh-14(ch3)* is not a fully penetrant AFD function switch, and it may still work weakly through AIB (Figure 5A). Nevertheless, a large proportion of the animals still display a cryophilic behavior that is not due to residual AFD function, since laser ablations and the triple mutant shows the same phenotype. This strongly suggests the existence of a second neural circuit as proposed by Hobert et al. (1997) and Mori and Ohshima (1995). Our data show that this circuit is normally overruled by the correct function of AFD-AIY-AIZ. Our results also show that, in contrast to the previous works, this second circuit seems to mediate a default cold-seeking behavior that is not mediated by AIZ exclusively. This circuit might constitute a survival strategy for the animal. Perhaps this second circuit also provides a reference for the AFD-AIY-AIZ circuitry (Figure 5B).

The AFD-AIY-AIZ thermosensory circuit mediates thermotaxis to warmer temperatures as default. These warmer temperatures are remembered as optimal because of a previous integration with information from other sensory functions like chemosensation (Hedgecock and Russell, 1975; Figure 5B). AFD mediates an adjustment of movement that is a consequence of constant signaling between sensory unit, memory, and motor output. Isothermal tracking results because AFD is able to measure not only temperature but also fast changes in temperature. The AFD signal is processed by AIY and AIZ, which also receive the food signals. The second, basic cryophilic thermosensory system seems to reside outside of the AFD-AIY-AIZ system and is only uncovered in the absence of AFD-AIY-AIZ.

An alternate hypothesis is that *ceh-14* regulates a memory function rather than thermosensation. This is not very likely since the memory function is clearly integrating food information with thermal input. Such a memory function is more likely to reside in interneurons, since they are supplied with information from several sources. AIY has been already hypothesized to be a possible memory-mediating interneuron (Hobert et al., 1997).

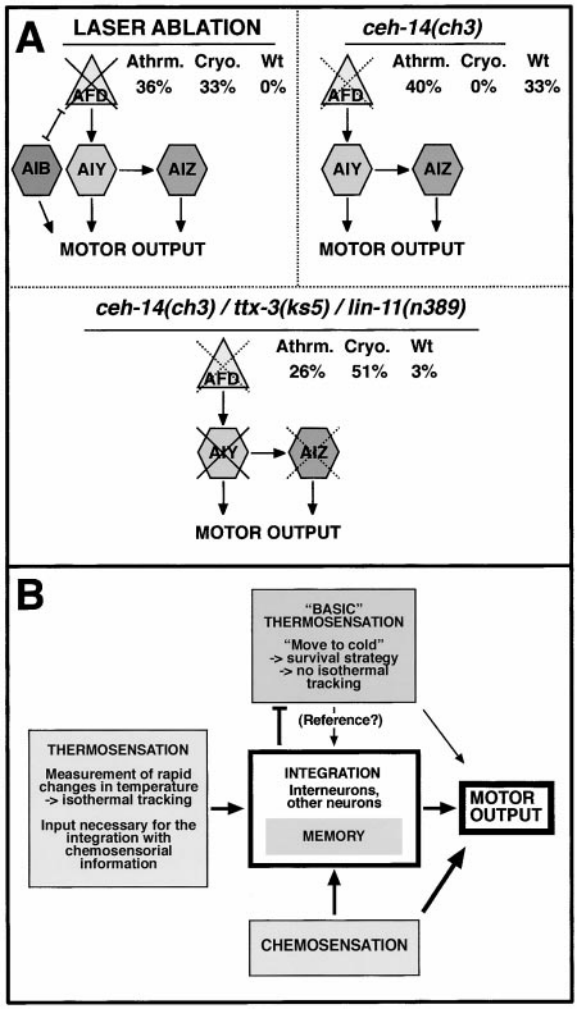

Figure 5. Model for the Function of Thermotaxis

(A) Comparison between the phenotypes of the laser ablation of AFD, the gene lesion *ceh-14(ch3)*, and the triple mutant *ceh-14(ch3) ttx-3(ks5) lin-11(n389)*. In summary, this panel shows that the animals are still cryophilic, whether AFD is removed by laser ablation or completely uncoupled from the motor output (triple mutant). This suggests that a "second" thermotaxis system distinct from AFD-AIY-AIZ exists. AFD is also connected via gap junctions to the interneuron AIB (shown only in the first scheme).

(B) Model for thermotaxis. Thermosensory and chemosensory cues are integrated and optimal conditions are memorized. A second basic cryophilic system serves as a reference for the primary thermophilic/isothermal tracking system and/or is overruled by the primary system under normal conditions (see Discussion for more details).

Genes Regulated by *ceh-14* Are Specifically Required for Thermosensation

We showed that *ceh-14* is required for correct thermotaxis mediated by AFD. To test whether *ceh-14* is sufficient, we misexpressed *ceh-14* in AWA and AWB, because they share some morphological features with AFD (Figure 3B), and they also share partially downstream interneurons (Figure 4A). Ectopic expression in a *ceh-14* mutant background was able to confer thermotactic behavior to populations of athermotactic animals in the case of AWB, but not in AWA (Figure 4B). It is not surprising that not all neurons are competent for particular

types of transformations. By all criteria that we tested, the function and morphology of the AWB neurons were not altered due to the ectopic expression of CEH-14. Chemotaxis behaviors to volatile agents that are specifically sensed by AWB are still normal. Confocal analysis using *gfp* markers did not reveal any morphological changes. Ectopic CEH-14 expression was also not able to cause ectopic expression of the AFD marker *gcy-8*. Thus, *ceh-14* does not substantially change the fate of these neurons, but a new function is added. Presently, given that no AFD markers regulated by *ceh-14* are known, it is not possible to prove to what extent AWB has been transformed into a thermosensory neuron at the molecular level.

Is it possible that one sensory neuron can be thermosensory and chemosensory? It is not known whether AFD can also sense some chemicals besides temperature. However, it has been suggested from laser ablation data that the lamellar cells (ALD) of the parasitic nematode *Strongyloides stercoralis* serves as a chemosensor and thermosensor (Ashton et al., 1999).

It has previously been shown that misexpression of the *odr-10* diacetyl receptor in the AWB neurons, which are responsible for avoidance to 2-nonanone, results in reprogramming so that diacetyl causes an inappropriate avoidance reaction (Troemel et al., 1997). One might have expected that the phenotype of lines misexpressing *ceh-14* in AWB is, for example, thermophilic. But, it has not been ruled out that AWB may direct attractive and avoidance behaviors depending on stimulus. Animals misexpressing *ceh-14* are not able to perform isothermal tracks on radial thermal gradients. These animals probably cannot fine tune body movement, because the thermal information is mediated by the inappropriate sensors that have different connections to interneurons and motor neurons, and *ceh-14* is not sufficient to induce major changes in cell fate.

The question is, what factors are transcriptionally regulated by *ceh-14* in AFD? These factors may fall into two categories: instructive or permissive for thermosensation. Instructive factors are proteins that are able to sense temperature and trigger the signaling cascade. They may also be factors that recruit proteins in such a way as to become functional in a thermosensory mechanism. They might also be "thermosensory" synaptic factors. Permissive proteins would include general cell–cell contact proteins, general signaling factors, synaptic factors, or even more general structural proteins. Our ectopic expression experiments suggest that the target genes of *ceh-14* are sufficient for thermosensation and therefore must be instructive. This is important also because no transcription factor has been described so far that is specifically involved in the differentiation of a thermosensory neuron. Thermosensation at physiological level is poorly understood in metazoans. Some *ceh-14* target(s) could be such novel "thermosensors."

Experimental Procedures

Constructs

General cloning procedures were performed according to Sambrook et al. (1989). pHK-107 is described as pPD95.69/*ceh-14* (first exon) in Cassata et al. (1998), and pHK-108 is derived from pPD95.67/*ceh-14* (full-length) by removing the NLS of the vector. pHK-108 was sequenced. The constructs for ectopic expression in AWA, pHK-131 and in AWB, pHK-141 were designed using the promoter regions of *odr-10* (Sengupta et al., 1996) and of *str-1* (Troemel et al., 1997), respectively. These promoter regions and the start codon of the respective gene were cloned according to Cassata et al. (1998) in the vector pPD95.75 and controlled for their ability to drive expression in the appropriate cells. Subsequently, the full-length cDNA of *ceh-14* was inserted into the promoter constructs by redesigning the start methionine and suppressing the stop codon by the same method in the first promoter constructs, sequenced and assayed for correct expression in worms. Details of cloning and sequences of all the oligonucleotides are available upon request.

Cloning of *ceh-14* cDNA

Using the predicted *ceh-14* ORF, two primers containing the start methionine and the stop codon were designed. With these, a cDNA was amplified from an embryonic cDNA library kindly provided by Dr. P. Okkema. This fragment was cloned into pKS Bluescript+ from Stratagene, sequenced, and is referred to as pKS-*ceh-14*. This partial cDNA was used as a probe to screen the same cDNA library according to Sambrook et al. (1989). Four independent clones were identified and sequenced. Additional 5′ UTR and the entire 3′ UTR sequences including a poly(A) tail were determined. The longest cDNA sequence has been submitted to GenBank.

Antibody Production and Antibody Immunolocalization

The 5′ BamHI–KpNI fragment of pKS-*ceh14* was subcloned into the bacterial expression vectors containing poly-histidine tags (Qiagen). Protein production was performed according to the instructions from the supplier. Rabbit anti-CEH-14 sera production was performed following standard procedures. The sera were affinity purified against a CEH-14 BamHI–XbaI amino-terminal fragment fused to GST using the vector pGEX-2T from AMRAD, following the protocol described by Burke et al. (1982). Immunolocalizations were performed according to Finney and Ruvkun (1990). Secondary antibodies used at 1:300 were Cy3-conjugated goat anti-rabbit IgG from Jackson Immuno Research.

Worm Strains

The strains used in this study are *C. elegans* Bristol strain (N2), YK11 [*mut-2 (r459)*; *dpy-19 (n1347)*; *ceh-14 (ms11::Tc1)*], *ceh-14(ch1)*, *ceh-14(ch3)*, FK134 [*ttx-3 (ks5)*], MT633 [*lin-11 (n389)*; *him-5 (e1467)*], CB3775 [*dpy-20(e2017)*], and TU900 [+/szT1 [*lon-2 (e678)*] uDf1/szT1].

ceh-14 Deletion Derivatives and Strain Construction

A Tc1 insertion in *ceh-14* was obtained by screening a Tc1 "library" using strain MT3126 [*mut-2* (r459); *dpy-19* (n1347)] (Greenstein et al., 1994). Two deletions in the *ceh-14* locus were obtained according to Zwaal et al. (1993) using the Tc1 insertion strain YK11. The molecular lesions in the two *ceh-14* deletion alleles called *ceh-14(ch1)* and *ceh-14(ch3)* were analyzed by sequencing the genomic portion around the breakpoints (Figure 1A). The deletion of *ceh-14(ch1)* lies entirely within the third intron; no adjacent coding sequence or splice sites are affected. In the larger deletion of *ceh-14(ch3)*, the loss includes the splice donor after the second exon, the entire second intron, the third exon, the third intron, and a portion of the fourth exon. The predicted ORF runs from exon 2 out of frame into exon 4 and leads to a premature stop codon after 12 new amino acids. This predicted protein product contains only part of the first LIM domain and should be nonfunctional (Figure 1B). To confirm the predictions, we sequenced RT-PCR products. *ceh-14(ch1)* produces a wild-type mRNA, and *ceh-14(ch3)* has the predicted deletion and frameshift. Northern blot analysis revealed that *ceh-14(ch1)* expresses normal amounts of *ceh-14* wild-type transcripts, whereas *ceh-14(ch3)* transcripts are reduced more than 7-fold (data not shown). This is probably due to loss of stability of the aberrant messenger RNA. CEH-14 protein is immunochemically detectable in *ceh-14(ch1)*, whereas no protein was detectable in *ceh-14(ch3)* animals (data not shown). This, taken together with the genetic data, shows that *ceh-14(ch3)* is a null allele.

In crossings the genotype of *ceh-14(ch1)* and *ceh-14(ch3)* was assayed by PCR. Double mutants TB530 [*ceh-14(ch3)*; *ttx-3(ks5)*] were tested using a separate set of primers for each mutant allele. Double and triple mutants containing *lin-11*(n389) were constructed

by crossing males from strain MT633 with the respective hermaphrodite and scoring F2 progeny for the *lin-11* Egl phenotype and the appropriate size PCR band for *ceh-14* and/or *ttx-3*. The penetrance of *ceh-14(ch3)* was assayed by crossing *ceh-14(ch3)* males with TU900 hermaphrodites containing the deletion uDF1, which includes the entire *ceh-14* locus. After mating, the F1 progeny was tested in isothermal tracking assays and afterwards scored by PCR for the *ceh-14(ch3)*.

Transgenic Strains

Transgenic lines were obtained by injecting the GFP constructs pHK-107, -108, -131, -141, *gcy-8* (Yu et al., 1997), and *tax-4* (Komatsu et al., 1996) into CB3775 [*dpy-20(e2017)*] or TB522 [*dpy-20(e2017)*; *ceh-14(ch3)*], coinjecting the *dpy-20* rescue marker pMH86 (Han and Sternberg, 1991) according to Mello et al. (1991). For the rescue of *ceh-14(ch3)*, six independent nonintegrated lines were assayed. The DNA concentrations used were 50 μg/ml for the *gfp* constructs and 20 μg/ml for marker constructs.

Transmission Electron Microscopy

Living young *ceh-14(ch3)* adults were prefixed in 3% paraformaldehyde, 0.25% glutaraldehyde for 1 hr and postfixed in 1% OsO_4 for another hour. Dehydration was performed with increasing concentrations of ethanol; the samples were embedded in EPON 512, and microtome sections were made according to standard procedures.

Behavioral Tests

Single worm thermotaxis assays were performed according to Mori and Ohshima (1995). The classification of the phenotypes was performed following the criteria shown therein, reduced and simplified as follows: wild type, W(+) plus C(+); intermediate, C/A(−) plus I(±); athermotactic, A(−); cryophilic, C(−); thermophilic, T(+) plus T(−).

Population thermotaxis assays were performed on a short, steep thermal gradient modified from Hedgecock and Russell (1975). Animals reared at 20°C were placed at the zone of 22°C on a small agar plate (5 cm) on which a reproducible linear temperature gradient from 10°C to 26°C had been induced (temperatures had been measured each 5 mm). After a fixed time (1 hr), the animals present in the colder (with respect to origin) or warmer region of the plate were scored. The thermotaxis index was calculated as follows: [(number of animals in cold area) − (number of animals in warm area)] / [total of animals that moved]. This test was validated using two mutants involved in the AFD-AIY axis [*ceh-14(ch3)* and *ttx-3(ks5)*, both show a predictable thermotaxis defect]. The assay therefore fullfills the requirements for a thermotaxis test. An average of 470 animals were tested per strain/line. They represent an average of six independent populations (plates). The standard error of the mean is derived from the number of populations tested.

Chemotaxis assays were performed according to Bargmann et al. (1993) for attraction and according to Troemel et al. (1997) for repulsion tests. An average of five populations were taken, ~100 worms each. The dilution of the chemicals used were (v/v): 1/1000 for diacetyl, trimethyldiazole, and 2-butanone, 1/10 for isoamyl alcohol and 2-nonanone, and 1/100 (w/v) for pyrazine.

Acknowledgments

We would like to thank Gisela Niklaus and Ursula Sauder for excellent technical support. We would also like to thank Peter Okkema, Cara Coburn, Cori Bargmann, and Andy Fire for sharing vectors, cDNAs, and libraries, and Cori Bargmann and Oliver Hobert for critical comments. Also, thanks to Franziska Kuhn for help with RNA and protein work and Eileen A. German for electron microscopy measurements. Some nematode strains were provided by the Caenorhabditis Genetics Center, which is funded by the National Institutes of Health (NIH) National Center for Research Resources. This work and H. K. have received support from the Novartis Foundation, from Jeff Schatz, and the Sandoz Stiftung. H. K. is a recipient of a JSPS Postdoctoral Fellowship for Research Abroad. T. R. B. is supported by grant NF. 3130-038786.93. D. H. H. and the Center for *C. elegans* Anatomy are funded by NIH grant RR12596. This work was supported by grants NF. 3100-040843.94 and NF. 31-50839.97 from the Swiss National Science Foundation and the University of Basel, Kanton Basel-Stadt.

Received December 28, 1999; revised February 3, 2000.

References

Agulnick, A.D., Taira, M., Breen, J.J., Tanaka, T., Dawid, I.B., and Westphal, H. (1996). Interactions of the LIM-domain-binding factor Ldb1 with LIM homeodomain proteins. Nature *384*, 270–272.

Appel, B., Korzh, V., Glasgow, E., Thor, S., Edlund, T., Dawid, I.B., and Eisen, J.S. (1995). Motoneuron fate specification revealed by patterned LIM homeobox gene expression in embryonic zebrafish. Development *121*, 4117–4125.

Ashton, F.T., Li, J., and Schad, G.A. (1999). Chemo- and thermosensory neurons: structure and function in animal parasitic nematodes. Vet. Parasitol. *84*, 297–316.

Bach, I., Carriere, C., Ostendorff, H.P., Andersen, B., and Rosenfeld, M.G. (1997). A family of LIM domain-associated cofactors confer transcriptional synergism between LIM and Otx homeodomain proteins. Genes Dev. *11*, 1370–1380.

Bargmann, C.I., Hartwieg, E., and Horvitz, H.R. (1993). Odorant-selective genes and neurons mediate olfaction in C. elegans. Cell *74*, 515–527.

Bürglin, T.R. (1995). The evolution of homeobox genes. In Biodiversity and Evolution, R. Arai, M. Kato, and Y. Doi, eds. (Tokyo: The National Science Museum Foundation), pp. 291–336.

Bürglin, T.R., Finney, M., Coulson, A., and Ruvkun, G. (1989). Caenorhabditis elegans has scores of homoeobox-containing genes. Nature *341*, 239–243.

Burke, B., Griffiths, G., Reggio, H., Louvard, D., and Warren, G. (1982). A monoclonal antibody against a 135-K Golgi membrane protein. EMBO J. *1*, 1621–1628.

Cassata, G., Kagoshima, H., Pretot, R.F., Aspock, G., Niklaus, G., and Bürglin, T.R. (1998). Rapid expression screening of Caenorhabditis elegans homeobox open reading frames using a two-step polymerase chain reaction promoter-gfp reporter construction technique. Gene *212*, 127–135.

Caterina, M.J., Rosen, T.A., Tominaga, M., Brake, A.J., and Julius, D. (1999). A capsaicin-receptor homologue with a high threshold for noxious heat. Nature *398*, 436–441.

Caterina, M.J., Schumacher, M.A., Tominaga, M., Rosen, T.A., Levine, J.D., and Julius, D. (1997). The capsaicin receptor: a heat-activated ion channel in the pain pathway. Nature *389*, 816–824.

C. elegans Sequencing Consortium (1998). Genome sequence of the nematode *C. elegans*: a platform for investigating biology. Science *282*, 2012–2018.

Coburn, C.M., and Bargmann, C.I. (1996). A putative cyclic nucleotide-gated channel is required for sensory development and function in C. elegans. Neuron *17*, 695–706.

Coburn, C.M., Mori, I., Ohshima, Y., and Bargmann, C.I. (1998). A cyclic nucleotide-gated channel inhibits sensory axon outgrowth in larval and adult Caenorhabditis elegans: a distinct pathway for maintenance of sensory axon structure. Development *125*, 249–258.

Colbert, H.A., Smith, T.L., and Bargmann, C.I. (1997). OSM-9, a novel protein with structural similarity to channels, is required for olfaction, mechanosensation, and olfactory adaptation in Caenorhabditis elegans. J. Neurosci. *17*, 8259–8269.

Dawid, I.B., Toyama, R., and Taira, M. (1995). LIM domain proteins. C. R. Acad. Sci. III *318*, 295–306.

Dawid, I.B., Breen, J.J., and Toyama, R. (1998). LIM domains: multiple roles as adapters and functional modifiers in protein interactions. Trends Genet. *14*, 156–162.

Finney, M., and Ruvkun, G. (1990). The *unc-86* gene product couples cell lineage and cell identity in C. elegans. Cell *63*, 895–905.

Greenstein, D., Hird, S., Plasterk, R.H., Andachi, Y., Kohara, Y., Wang, B., Finney, M., and Ruvkun, G. (1994). Targeted mutations in the Caenorhabditis elegans POU homeo box gene *ceh-18* cause

defects in oocyte cell cycle arrest, gonad migration, and epidermal differentiation. Genes Dev. *8*, 1935–1948.

Han, M., and Sternberg, P.W. (1991). Analysis of dominant-negative mutations of the Caenorhabditis elegans *let-60* ras gene. Genes Dev. *5*, 2188–2198.

Hedgecock, E.M., and Russell, R.L. (1975). Normal and mutant thermotaxis in the nematode Caenorhabditis elegans. Proc. Natl. Acad. Sci. USA *72*, 4061–4065.

Hobert, O., Mori, I., Yamashita, Y., Honda, H., Ohshima, Y., Liu, Y., and Ruvkun, G. (1997). Regulation of interneuron function in the C. elegans thermoregulatory pathway by the *ttx-3* LIM homeobox gene. Neuron *19*, 345–357.

Hobert, O., D'Alberti, T., Liu, Y., and Ruvkun, G. (1998). Control of neural development and function in a thermoregulatory network by the LIM homeobox gene *lin-11*. J. Neurosci. *18*, 2084–2096.

Jurata, L.W., Kenny, D.A., and Gill, G.N. (1996). Nuclear LIM interactor, a rhombotin and LIM homeodomain interacting protein, is expressed early in neuronal development. Proc. Natl. Acad. Sci. USA *93*, 11693–11698.

Kalionis, B., and O'Farrell, P.H. (1993). A universal target sequence is bound in vitro by diverse homeodomains. Mech. Dev. *43*, 57–70.

Komatsu, H., Mori, I., Rhee, J.S., Akaike, N., and Ohshima, Y. (1996). Mutations in a cyclic nucleotide-gated channel lead to abnormal thermosensation and chemosensation in C. elegans. Neuron *17*, 707–718.

Lundgren, S.E., Callahan, C.A., Thor, S., and Thomas, J.B. (1995). Control of neuronal pathway selection by the Drosophila LIM homeodomain gene *apterous*. Development *121*, 1769–1773.

Mello, C.C., Kramer, J.M., Stinchcomb, D., and Ambros, V. (1991). Efficient gene transfer in C. elegans: extrachromosomal maintenance and integration of transforming sequences. EMBO J. *10*, 3959–3970.

Mori, I., and Ohshima, Y. (1995). Neural regulation of thermotaxis in Caenorhabditis elegans. Nature *376*, 344–348.

Perkins, L.A., Hedgecock, E.M., Thomson, J.N., and Culotti, J.G. (1986). Mutant sensory cilia in the nematode Caenorhabditis elegans. Dev. Biol. *117*, 456–487.

Pfaff, S.L., Mendelsohn, M., Stewart, C.L., Edlund, T., and Jessell, T.M. (1996). Requirement for LIM homeobox gene Isl1 in motor neuron generation reveals a motor neuron-dependent step in interneuron differentiation. Cell *84*, 309–320.

Sagasti, A., Hobert, O., Troemel, E.R., Ruvkun, G., and Bargmann, C.I. (1999). Alternative olfactory neuron fates are specified by the LIM homeobox gene lim-4. Genes Dev. *13*, 1794–1806.

Sambrook, J., Fritsch, E.F., and Maniatis, T. (1989). Molecular Cloning: A Laboratory Manual, Second Edition (Cold Spring Harbor, NY: Cold Spring Harbor Laboratory Press).

Sengupta, P., Chou, J.H., and Bargmann, C.I. (1996). odr-10 encodes a seven transmembrane domain olfactory receptor required for responses to the odorant diacetyl. Cell *84*, 899–909.

Sharma, K., Sheng, H.Z., Lettieri, K., Li, H., Karavanov, A., Potter, S., Westphal, H., and Pfaff, S.L. (1998). LIM homeodomain factors Lhx3 and Lhx4 assign subtype identities for motor neurons. Cell *95*, 817–828.

Thor, S., and Thomas, J.B. (1997). The Drosophila *islet* gene governs axon pathfinding and neurotransmitter identity. Neuron *18*, 397–409.

Thor, S., Andersson, S.G., Tomlinson, A., and Thomas, J.B. (1999). A LIM-homeodomain combinatorial code for motor-neuron pathway selection. Nature *397*, 76–80.

Troemel, E.R., Kimmel, B.E., and Bargmann, C.I. (1997). Reprogramming chemotaxis responses: sensory neurons define olfactory preferences in C. elegans. Cell *91*, 161–169.

Tsuchida, T., Ensini, M., Morton, S.B., Baldassare, M., Edlund, T., Jessell, T.M., and Pfaff, S.L. (1994). Topographic organization of embryonic motor neurons defined by expression of LIM homeobox genes. Cell *79*, 957–970.

Varela-Echavarria, A., Pfaff, S.L., and Guthrie, S. (1996). Differential expression of LIM homeobox genes among motor neuron subpopulations in the developing chick brain stem. Mol. Cell. Neurosci. *8*, 242–257.

Way, J.C., and Chalfie, M. (1988). *mec-3*, a homeobox-containing gene that specifies differentiation of the touch receptor neurons in C. elegans. Cell *54*, 5–16.

Way, J.C., and Chalfie, M. (1989). The mec-3 gene of Caenorhabditis elegans requires its own product for maintained expression and is expressed in three neuronal cell types. Genes Dev. *3*, 1823–1833.

White, J.G., Southgate, E., Thomson, J.N., and Brenner, S. (1986). The structure of the nervous system of the nematode *Caenorhabditis elegans*. Philos. Trans. R. Soc. Lond. B Biol. Sci. *314*, 1–340.

Yu, S., Avery, L., Baude, E., and Garbers, D.L. (1997). Guanylyl cyclase expression in specific sensory neurons: a new family of chemosensory receptors. Proc. Natl. Acad. Sci. USA *94*, 3384–3387.

Zwaal, R.R., Broeks, A., van Meurs, J., Groenen, J.T., and Plasterk, R.H. (1993). Target-selected gene inactivation in Caenorhabditis elegans by using a frozen transposon insertion mutant bank. Proc. Natl. Acad. Sci. USA *90*, 7431–7435.

GenBank Accession Number

The GenBank accession number for the sequence discussed in this paper is AF244368.